PROCEEDINGS OF SCIENCE

PoS(QCHSC24)067

Electromagnetic properties and hadron structures

Zhan-Wei Liu[a,b,c,*]

[a] *School of Physical Science and Technology, Lanzhou University, Lanzhou 730000, China*

[b] *Research Center for Hadron and CSR Physics, Lanzhou University and Institute of Modern Physics of CAS, Lanzhou 730000, China*

[c] *Lanzhou Center for Theoretical Physics, MoE Frontiers Science Center for Rare Isotopes, Key Laboratory of Quantum Theory and Applications of MoE, Key Laboratory of Theoretical Physics of Gansu Province, Gansu Provincial Research Center for Basic Disciplines of Quantum Physics, Lanzhou University, Lanzhou 730000, China*

E-mail: liuzhanwei@lzu.edu.cn

In this report, we focus on the electromagnetic properties of hadrons which can help us understand the structures of resonances. We review our works about the radiative decays of $D^*_{s0}(2317)$, $D'_{s1}(2460)$, and $X(3872)$ where the molecule components play important roles. We discuss the final-state interaction effects in the electron-positron annihilation processes and compare with new experimental data.

The XVIth Quark Confinement and the Hadron Spectrum Conference (QCHSC24)
19-24 August, 2024
Cairns Convention Centre, Cairns, Queensland, Australia

*Speaker

Electromagnetic interaction is very important for disclosing the structures of hadrons. The magnetic moments of nucleons are very different from that of the electron, which reflects that the nucleons are not point-like particles. The deep-inelastic scattering processes told us that the nucleons are much more complex than the naive quark model predictions.

The magnetic moments of the exotic states were also widely studied. Those of the hidden-charmed pentaquark states were discussed with the molecule, diquark-triquark and other configurations within quark model and QCD sum rules [1–3]. The coupled channel effects and the D wave contributions were further investigated, and the former would lead to 0.1~0.4 μ_N change while the latter induces the variation of less than 0.03 μ_N for the magnetic moments of P_c states [4]. The measurement of the magnetic moments in future would help us distinguish different models.

The photoproduction processes are also helpful to study the structures of resonance through electromagnetic interactions. They have been studied within chiral perturbation theory, dynamical coupled-channel models, lattice QCD, and so on [5–12]. Recently, pion photoproduction of nucleon excited states has been investigated within Hamiltonian effective field theory where the multipole amplitudes E_{0+} and M_{1-} are calculated [13, 14], which shows the triquark components in $N(1535)$ and $N(1650)$ are important while the contribution from the positive bare state is small.

Radiative decays can easily reveal that the real resonance structures are more different from the naive quark model since those of traditional hadrons can be obtained more reliably from theory. Multiquark components usually would give certain corrections to explain the relevant experiments. For example, $\Delta(1232) \to N\gamma$ can be studied well with the $\Delta(1232)$ interpreted as a triquark core plus $N\pi$ etc [15, 16].

In this report we first shortly reviewed the radiative decays of $D^*_{s0}(2317)$, $D'_{s1}(2460)$, and $X(3872)$ in Sec. 1. We focus on the electromagnetic processes of $e^+e^- \to p\bar{p}, \Lambda_c\bar{\Lambda}_c$ in Sec. 2.

1. Radiative decays

In 2003, the *BABAR* Collaboration observed the $D^*_{s0}(2317)$ [17] and the CLEO Collaboratio found $D'_{s1}(2460)$ [18]. Since their discoveries, different interpretations were provided to explain their masses. Some work with the $c\bar{s}$ picture give the obtained masses were a little bigger than the experimental data, and thus the very close $D^{(*)}K$ channels are important for them. The radiative transitions for conventional D_s mesons were explored in Refs. [19–29], and those for the conventional quark-antiquark and four-quark mixtures were studied in Refs. [30, 31]. Within the molecular picture, the processes of $D^*_{s0}(2317) \to D^*_s\gamma$, $D'_{s1}(2460) \to D^*_s\gamma$, $D'_{s1}(2460) \to D^*_{s0}(2317)\gamma$ were studied in Refs. [32–39].

In Ref. [40] we studied the masses of $D^*_{s0}(2317)$ and $D'_{s1}(2460)$ with three scenarios as shown in Fig. 1. We considered both the coupling between $c\bar{s}$ and $D^{(*)}K$ and the $D^{(*)}K$-$D^{(*)}K$ interaction. From the figure, we can see that the naive quark model gives the mass (green dotted lines) is larger than the experimental one. The coupled channel effect (blue dashed lines), just with the $c\bar{s}$-$D^{(*)}K$ coupling, can lower the theoretical mass. After adding the $D^{(*)}K$-$D^{(*)}K$ interaction (red solid lines), the obtained masses can fit the observation.

In addition to the difference of the mass spectrum, we further discussed the decay behavior of the $D^*_{s0}(2317)$ and $D'_{s1}(2460)$ with different configurations [40]. For the $D^*_{s0}(2317) \to D^*_s\gamma$ partial decay width, the pure molecule assumption would predict it is about 10~40 keV while the

PoS(QCHSC24)067

mixing of the $c\bar{s}$ and DK picture gives about 1∼5 keV. Thus the study of radiative decays may help us to distinguish the structures of the resonances.

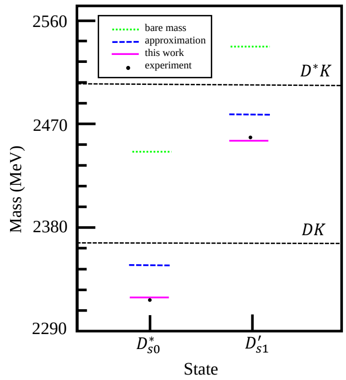

Figure 1: Comparison for the masses of $D^*_{s0}(2317)$ and $D'_{s1}(2460)$ with different scenarios. The green dotted lines represent the results of naive quark model, the blue dashed lines are obtained with the coupling between the $c\bar{s}$ and $D^{(*)}K$ states considered, and after adding the $D^{(*)}K$-$D^{(*)}K$ interaction one gets the red solid lines.

There is a long debate on the structure of $X(3872)$. Its mass is close to the $D\bar{D}^*$ threshold, and thus the molecule interpretation becomes popular. However, the charmonium structure cannot be excluded. In 2004, a small ratio $R_{\gamma\psi}$ in the molecular picture was predicted compared to that with the charmonium assumption [41]. Later $R_{\gamma\psi}$ was measured in experiments but with obvious differences among different groups [42–45],

$$R_{\gamma\psi} = \frac{\mathcal{B}[X(3872)\to\gamma\psi(2S)]}{\mathcal{B}[X(3872)\to\gamma J/\psi]} \begin{cases} = 3.4\pm 1.4\ (3.5\sigma) & \text{BaBar} \\ = 2.46\pm 0.64\pm 0.29\ (4.4\sigma) & \text{LHCb} \\ <\ 2.1\ (90\%\ \text{C.L.}) & \text{Belle} \\ <\ 0.59\ (90\%\ \text{C.L.}) & \text{BESIII} \end{cases}.$$

The charmonium structure can explain some above experiments naturally. However, molecular interpretation cannot be excluded [46]. With the improvement of the $X(3872)$ mass study, we carefully examined the radiative decay of $X(3872)$ in the molecular picture [47].

We studied the binding energy of $D\bar{D}^*$ molecules with the isospin breaking, coupled channel, and Coulomb interaction effects [47], which can give precise wavefunction for $X(3872)$. With this wavefunction $\hat{\phi}^{JM}_{[AB]}(\mathbf{p})$, we further calculated the scattering amplitudes $\hat{\mathcal{M}}_{AB\to CD}$ in Fig. 2 and obtained the decay amplitude $\mathcal{M}^{JM}_{[AB]\to CD}$ of the molecule $[AB]$ through

$$\mathcal{M}^{JM}_{[AB]\to CD} = \frac{\sqrt{2m_{[AB]}}}{\sqrt{2m_A}\sqrt{2m_B}}\int\frac{\mathrm{d}^3\mathbf{p}}{(2\pi)^{3/2}}\,\hat{\phi}^{JM}_{[AB]}(\mathbf{p})\otimes\hat{\mathcal{M}}_{AB\to CD}, \tag{1}$$

which gives the relevant decay width $\Gamma_{[AB]\to CD}$

$$\Gamma_{[AB]\to CD} = \frac{1}{3}\frac{|\mathbf{k}|}{32\pi^2 m_X^2}\sum_M\int\left|\mathcal{M}^{JM}_{[AB]\to CD}\right|^2\mathrm{d}\Omega_{\mathbf{k}}. \tag{2}$$

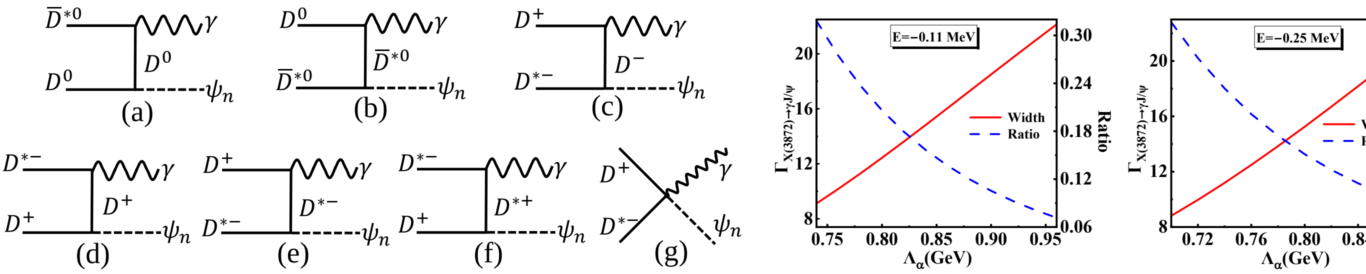

Figure 2: On the left are the Feynman diagrams for the transitions $X(3872) \to \gamma\psi_n$ when the $X(3872)$ is a $D\bar{D}^*$ hadronic molecule with $J^{PC} = 1^{++}$. The conjugated diagrams are not shown, but are included in the calculations.
The right graph gives the radiative decay width of the $X(3872) \to \gamma J/\psi$ and the ratio $R_{\gamma\psi} = \frac{\Gamma_{X(3872)\to\gamma\psi(2S)}}{\Gamma_{X(3872)\to\gamma J/\psi}}$ for the binding energy $E = -0.11$ MeV. The units of the radiative decay width are keV.

As shown in the right graph of Fig. 2, the ratio $R_{\gamma\psi}$ is about 0.05~0.30. Our results are consistent with the Belle and BESIII measurements.

2. Final state interaction in the electron-positron annihilation processes

The timelike electromagnetic form factors of nucleons are closely related to the electron-positron annihilation processes, and there are oscillation behaviors in them [48], which can also be seen in the left graph in Fig. 3. This damped oscillation phenomenon were studied with various mechanisms [49–53].

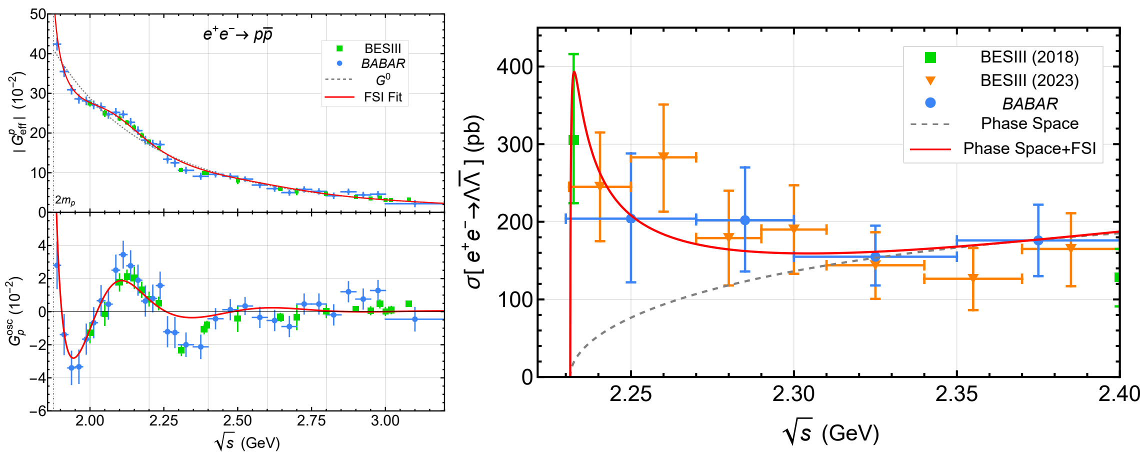

Figure 3: The left graph gives the effective form factors for protons in the timelike region. At the top are the effective form factors $|G_{\text{eff}}|$, while at the bottom is the oscillation part G^{osc} after subtracting the smooth background part G_0 (gray dashed line). The threshold positions $\sqrt{s} = 2m_N$ are marked as gray dot-dashed vertical lines. In the figure, we include BESIII [54] (green square) and *BABAR* [48] (blue circle) data for $p\bar{p}$. The right graph are about the cross sections near the thresholds for $e^+e^- \to \Lambda\bar{\Lambda}$ [55–57]. If the cross section is proportional to the phase space, the fit is shown as the gray dashed line. After considering the final state interaction effect, the red solid line can explain the threshold enhancement phenomenon.

With a simple square-well potential for the final-state interaction of $N\bar{N}$, we can obtain their zero-point wavefunctions with quantum mechanics, which can provide a correction factor for the cross sections or the form factors [58]. Using this final-state interaction effect, we can explain the damped oscillation behavior well as shown in the left graph of Fig. 3.

The threshold enhancement phenomenon of $e^+e^- \to \Lambda\bar{\Lambda}$ can be clearly seen in the right graph of Fig. 3. With the same final-state interaction effect, we can fit the experimental data before 2020 well. We notice that the BESIII collaboration reported their new measurement on the cross section of $e^+e^- \to \Lambda\bar{\Lambda}$ via ISR [57]. As shown in the right graph of Fig. 3, the new data are consistent with our earlier description.

Acknowledgment

The author expresses sincere acknowledgment to the following collaborators over the years spent on this topic: Xu Cao, Ping Chen, Rui Chen, Dan Guo, Zhi-Hui Guo, Derek B. Leinweber, Hao-Song Li, Ming-Wei Li, Xiang Liu, Si-Qiang Luo, Lu Meng, Zhi-Feng Sun, Anthony W. Thomas, Ri-Qing Qian, Guang-Juan Wang, Fu-Lai Wang, Jun-Zhang Wang, Zi-Le Zhang, Shi-Lin Zhu, Yu Zhuge and so on. This project is supported by the National Natural Science Foundation of China under Grants No. 12175091, No. 12335001, and No. 12247101, the Fundamental Research Funds for the Central Universities under Grant No. lzujbky-2024-jdzx06, the Natural Science Foundation of Gansu Province under Grants No. 22JR5RA389 and No. 25JRRA799, the '111 Center' under Grant No. B20063, and the innovation project for young science and technology talents of Lanzhou city under Grant No. 2023-QN-107.

References

[1] G.-J. Wang, et al., Magnetic moments of the hidden-charm pentaquark states, Phys. Rev. D 94 (2016) 094018.

[2] U. Özdem, Magnetic dipole moments of the hidden-charm pentaquark states: $P_c(4440)$, $P_c(4457)$ and $P_{cs}(4459)$, Eur. Phys. J. C 81 (2021) 277.

[3] Y.-J. Xu, Y.-L. Liu, and M.-Q. Huang, The magnetic moment of $P_c(4312)$ as a $\bar{D}\Sigma_c$ molecular state, Eur. Phys. J. C 81 (2021) 421.

[4] M.-W. Li, Z.-W. Liu, Z.-F. Sun, and R. Chen, Magnetic moments and transition magnetic moments of Pc and Pcs states, Phys. Rev. D 104 (2021) 054016.

[5] V. Bernard, N. Kaiser, J. Gasser, and U. G. Meissner, Neutral pion photoproduction at threshold, Phys. Lett. B 268 (1991) 291.

[6] M. Mai, P. C. Bruns, and U.-G. Meissner, Pion photoproduction off the proton in a gauge-invariant chiral unitary framework, Phys. Rev. D 86 (2012) 094033.

[7] M. Hilt, S. Scherer, and L. Tiator, Threshold π^0 photoproduction in relativistic chiral perturbation theory, Phys. Rev. C 87 (2013) 045204.

[8] B. Julia-Diaz, T. S. H. Lee, T. Sato, and L. C. Smith, Extraction and Interpretation of gamma N —> Delta Form Factors within a Dynamical Model, Phys. Rev. C 75 (2007) 015205.

[9] M. Doring, et al., Analytic properties of the scattering amplitude and resonances parameters in a meson exchange model, Nucl. Phys. A 829 (2009) 170.

[10] D. Rönchen, M. Döring, U.-G. Meißner, and C.-W. Shen, Light baryon resonances from a coupled-channel study including **KΣ** photoproduction, Eur. Phys. J. A 58 (2022) 229.

[11] V. V. Anisovich, et al.: Mesons and baryons: Systematization and methods of analysis (2008).

[12] A. V. Anisovich et al., The impact of new polarization data from Bonn, Mainz and Jefferson Laboratory on $\gamma p \to \pi N$ multipoles, Eur. Phys. J. A 52 (2016) 284.

[13] D. Guo and Z.-W. Liu, Pion photoproduction off nucleon with Hamiltonian effective field theory, Phys. Rev. D 105 (2022) 114039.

[14] Y. Zhuge, Z.-W. Liu, D. B. Leinweber, and A. W. Thomas, Pion photoproduction of nucleon excited states with Hamiltonian effective field theory, Phys. Rev. D 110 (2024) 094015.

[15] D.-H. Lu, A. W. Thomas, and A. G. Williams, A Chiral bag model approach to delta electroproduction, Phys. Rev. C 55 (1997) 3108.

[16] H.-S. Li, L. Meng, Z.-W. Liu, and S.-L. Zhu, Radiative decays of the doubly charmed baryons in chiral perturbation theory, Phys. Lett. B 777 (2018) 169.

[17] B. Aubert et al. (BaBar), Observation of a narrow meson decaying to $D_s^+\pi^0$ at a mass of 2.32-GeV/c^2, Phys. Rev. Lett. 90 (2003) 242001.

[18] D. Besson et al. (CLEO), Observation of a narrow resonance of mass 2.46-GeV/c**2 decaying to D*+(s) pi0 and confirmation of the D*(sJ)(2317) state, Phys. Rev. D 68 (2003) 032002 [Erratum: Phys.Rev.D 75, 119908 (2007)].

[19] S. Godfrey, Testing the nature of the D(sJ)*(2317)+ and D(sJ)(2463)+ states using radiative transitions, Phys. Lett. B 568 (2003) 254.

[20] S. Godfrey, K. Moats, and E. S. Swanson, B and B_s Meson Spectroscopy, Phys. Rev. D 94 (2016) 054025.

[21] Q.-F. Lü, et al., Excited bottom and bottom-strange mesons in the quark model, Phys. Rev. D 94 (2016) 074012.

[22] S. Godfrey and K. Moats, Properties of Excited Charm and Charm-Strange Mesons, Phys. Rev. D 93 (2016) 034035.

[23] Q. Li, et al., Excited bottom-charmed mesons in a nonrelativistic quark model, Phys. Rev. D 99 (2019) 096020.

[24] S. F. Radford, W. W. Repko, and M. J. Saelim, Potential model calculations and predictions for c anti-s quarkonia, Phys. Rev. D 80 (2009) 034012.

[25] S.-F. Chen, J. Liu, H.-Q. Zhou, and D.-Y. Chen, Electric transitions of the charmed-strange mesons in a relativistic quark model, Eur. Phys. J. C 80 (2020) 290.

[26] N. Green, W. W. Repko, and S. F. Radford, Note on predictions for $c\bar{s}$ quarkonia using a three-loop static potential, Nucl. Phys. A 958 (2017) 71.

[27] S. Godfrey, Properties of the charmed P-wave mesons, Phys. Rev. D 72 (2005) 054029.

[28] P. Colangelo, F. De Fazio, and A. Ozpineci, Radiative transitions of D*(sJ)(2317) and D(sJ)(2460), Phys. Rev. D 72 (2005) 074004.

[29] M. F. M. Lutz and M. Soyeur, Radiative and isospin-violating decays of D(s)-mesons in the hadrogenesis conjecture, Nucl. Phys. A 813 (2008) 14.

[30] J. Vijande, F. Fernandez, and A. Valcarce, Open-charm meson spectroscopy, Phys. Rev. D 73 (2006) 034002 [Erratum: Phys.Rev.D 74, 059903 (2006)].

[31] J. Vijande, A. Valcarce, and F. Fernandez, B meson spectroscopy, Phys. Rev. D 77 (2008) 017501.

[32] M. Cleven, et al., Strong and radiative decays of the $D_{s0}^*(2317)$ and $D_{s1}(2460)$, Eur. Phys. J. A 50 (2014) 149.

[33] H.-L. Fu, et al., Update on strong and radiative decays of the $D_{s0}^*(2317)$ and $D_{s1}(2460)$ and their bottom cousins, Eur. Phys. J. A 58 (2022) 70.

[34] A. Faessler, T. Gutsche, V. E. Lyubovitskij, and Y.-L. Ma, Strong and radiative decays of the D(s0)*(2317) meson in the DK-molecule picture, Phys. Rev. D 76 (2007) 014005.

[35] A. Faessler, T. Gutsche, V. E. Lyubovitskij, and Y.-L. Ma, D* K molecular structure of the D(s1)(2460) meson, Phys. Rev. D 76 (2007) 114008.

[36] c.-J. Xiao, D.-Y. Chen, and Y.-L. Ma, Radiative and pionic transitions from the $D_{s1}(2460)$ to the $D_{s0}^*(2317)$, Phys. Rev. D 93 (2016) 094011.

[37] G.-Q. Feng and X.-H. Guo, DK molecule in the Bethe-Salpeter equation approach in the heavy quark limit, Phys. Rev. D 86 (2012) 036004.

[38] G. Q. Feng, X. H. Guo, and Z. H. Zhang, Studying the D* K molecular structure of D/s(2460) in the Bethe-Salpeter approach, Eur. Phys. J. C 72 (2012) 2033.

[39] D. Gamermann, L. R. Dai, and E. Oset, Radiative decay of the dynamically generated open and hidden charm scalar meson resonances D(s0)*(2317) and X(3700), Phys. Rev. C 76 (2007) 055205.

[40] Z.-L. Zhang, et al., Masses and radiative decay widths of Ds0*(2317) and Ds1'(2460) and their bottom analogs, Phys. Rev. D 110 (2024) 094037.

[41] E. S. Swanson, Diagnostic decays of the X(3872), Phys. Lett. B 598 (2004) 197.

[42] R. Aaij et al. (LHCb), Evidence for the decay $X(3872) \to \psi(2S)\gamma$, Nucl. Phys. B 886 (2014) 665.

[43] V. Bhardwaj et al. (Belle), Observation of $X(3872) \to J/\psi\gamma$ and search for $X(3872) \to \psi'\gamma$ in B decays, Phys. Rev. Lett. 107 (2011) 091803.

[44] M. Ablikim et al. (BESIII), Study of Open-Charm Decays and Radiative Transitions of the $X(3872)$, Phys. Rev. Lett. 124 (2020) 242001.

[45] B. Aubert et al. (BaBar), Evidence for $X(3872) \to \psi_{2S}\gamma$ in $B^\pm \to X_{3872}K^\pm$ decays, and a study of $B \to c\bar{c}\gamma K$, Phys. Rev. Lett. 102 (2009) 132001.

[46] F.-K. Guo, et al., What can radiative decays of the X(3872) teach us about its nature?, Phys. Lett. B 742 (2015) 394.

[47] P. Chen, et al., Role of electromagnetic interactions in the X(3872) and its analogs, Phys. Rev. D 109 (2024) 094002.

[48] A. Bianconi and E. Tomasi-Gustafsson, Periodic interference structures in the timelike proton form factor, Phys. Rev. Lett. 114 (2015) 232301.

[49] X. Cao, J.-P. Dai, and H. Lenske, Timelike nucleon electromagnetic form factors: All about interference of isospin amplitudes, Phys. Rev. D 105 (2022) L071503.

[50] I. T. Lorenz, H. W. Hammer, and U. G. Meißner, New structures in the proton-antiproton system, Phys. Rev. D 92 (2015) 034018.

[51] A. Bianconi and E. Tomasi-Gustafsson, Phenomenological analysis of near threshold periodic modulations of the proton timelike form factor, Phys. Rev. C 93 (2016) 035201.

[52] Q.-H. Yang, et al., New insights into the oscillations of the nucleon electromagnetic form factors, Sci. Bull. 68 (2023) 2729.

[53] Z.-Y. Li, A.-X. Dai, and J.-J. Xie, Electromagnetic Form Factors of Λ Hyperon in the Vector Meson Dominance Model and a Possible Explanation of the Near-Threshold Enhancement of the Reaction, Chin. Phys. Lett. 39 (2022) 011201.

[54] M. Ablikim et al. (BESIII), Measurement of proton electromagnetic form factors in $e^+e^- \to p\bar{p}$ in the energy region 2.00 - 3.08 GeV, Phys. Rev. Lett. 124 (2020) 042001.

[55] M. Ablikim et al. (BESIII), Observation of a cross-section enhancement near mass threshold in $e^+e^- \to \Lambda\bar{\Lambda}$, Phys. Rev. D 97 (2018) 032013.

[56] B. Aubert et al. (BaBar), Study of $e^+e^- \to \Lambda\bar{\Lambda}$, $\Lambda\bar{\Sigma}^0$, $\Sigma^0\bar{\Sigma}^0$ using initial state radiation with BABAR, Phys. Rev. D 76 (2007) 092006.

[57] M. Ablikim et al. (BESIII), Measurement of the $e^+e^- \to \Lambda\bar{\Lambda}$ cross section from threshold to 3.00 GeV using events with initial-state radiation, Phys. Rev. D 107 (2023) 072005.

[58] R.-Q. Qian, Z.-W. Liu, X. Cao, and X. Liu, Toy model to understand the oscillatory behavior in timelike nucleon form factors, Phys. Rev. D 107 (2023) L091502.

PoS(QCHSC24)067